

## 5 MW 고온초전도 모터 설계

### Conceptual Design of a 5 MW HTS Motor

백승규<sup>1\*</sup>, 권영길<sup>1</sup>, 김호민<sup>1</sup>, 이재득<sup>2</sup>, 김영춘<sup>3</sup>, 박희주<sup>3</sup>, 권운식<sup>3</sup>, 박관수<sup>4</sup>

S. K. Baik<sup>1\*</sup>, Y. K. Kwon<sup>1</sup>, H. M. Kim<sup>1</sup>, J. D. Lee<sup>2</sup>,  
Y. C. Kim<sup>3</sup>, H. J. Park<sup>3</sup>, W. S. Kwon<sup>3</sup>, and G. S. Park<sup>4</sup>

**Abstract:** The superconducting motor shows several advantages such as smaller size and higher efficiency against conventional motor especially utilized in ship propulsion application. However, this size reduction merit appears in large capacity more than several MW. We are going to develop a 5 MW class synchronous motor with rotating High-Temperature Superconducting (HTS) coil, that is aimed to be utilized for ship propulsion so it has very low-speed. The ship propulsion motor must generate very high electromagnetic torque instead of low-speed. Therefore, the rotor (field) coils need very large magnetic flux that results in large amount of expensive HTS conductor for the field coil. In this paper a 5 MW HTS motor for ship propulsion is considered to be designed with construction cost reduced via HTS field coil cost reduction because HTS conductor cost is critical factor in the construction cost of HTS motor. In order to reduce the HTS conductor amount, iron-cored rotor types are considered, so several cases with iron-core are compared one another and with an air-core case.

**Key Words:** superconducting motor, smaller size, higher efficiency, ship propulsion, HTS conductor amount, iron-cored rotor.

## 1. INTRODUCTION

It is expected that the first commercial application of HTS motor will be marine transportation. Especially weight and size reduction in electrical propulsion systems of navy and commercial vessels increases design flexibility to bring critical benefits. Electrical propulsion system has already penetrated into cruise ship market due to advantages over mechanical propulsion systems. Beside of other merits the HTS based ship propulsion system is

more attractive in electrical propulsion system because of improved power density and operation efficiency. In this paper a 5 MW class HTS synchronous motor with a rotating HTS field coil is considered for design aimed to application such as navy vessels and submarines[1].

The cross-sectional structure of rotating HTS field type synchronous motor is shown in Fig. 1, where the machine shield plays a role in confining magnetic field within a machine. The HTS field coil generates direct current magnetic field but the armature coils flow alternating current which brings out rotating magnetic field to pull the HTS field coil into the same rotating speed. The armature coils are inserted into non-magnetic support material such as FRP (Fiberglass Reinforced Plastic).

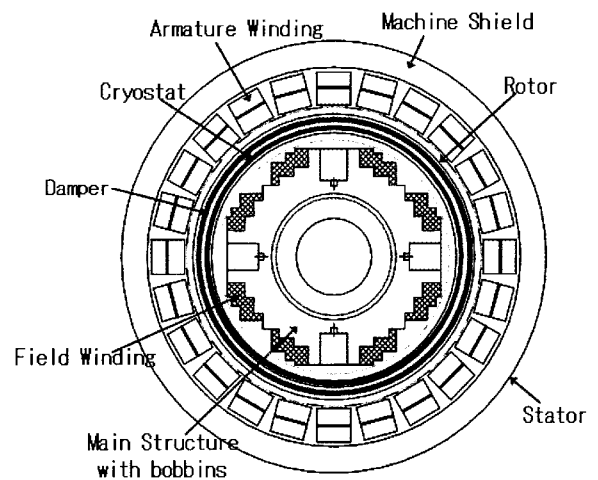


Fig. 1. Cross-sectional structure of rotating field type superconducting motor.

## 2. 5 MW ROTATING FIELD TYPE HTS MOTOR DESIGN

### 2.1. Air-cored Type Design

The conventional motor has iron-cored structure both at the field coil part and at the armature coil part, so it has very small air-gap between the field and the armature. However, the air-cored type HTS motor has iron just at the machine shield shown in

<sup>1</sup>정 회 원 : 한국전기연구원 초전도기기연구그룹

<sup>2</sup>학생회원 : 한국전기연구원 초전도기기연구그룹

<sup>3</sup>정 회 원 : 두산중공업 기술연구원

<sup>4</sup>비 회 원 : 부산대학교 전자 전기 컴퓨터 공학부

\*교신저자 : skbaik@keri.re.kr

원고접수 : 2008년 09월 11일

심사완료 : 2008년 09월 19일

게재확정 : 2008년 09월 19일

Fig. 1 as a cylindrical structure stacked by silicon steel sheets. Due to the structure without iron teeth and slots, it is possible to establish mathematical equations of magnetic field distribution and design parameters in the superconducting motor and generator. A design program algorithm composed of the established equations is shown in Fig. 2 and the program result brings out many design parameters such as dimensions of each part and coil turn numbers. This superconducting motor design program is based on Laplace equation established in 2 dimensional cylindrical coordinate[2-3].

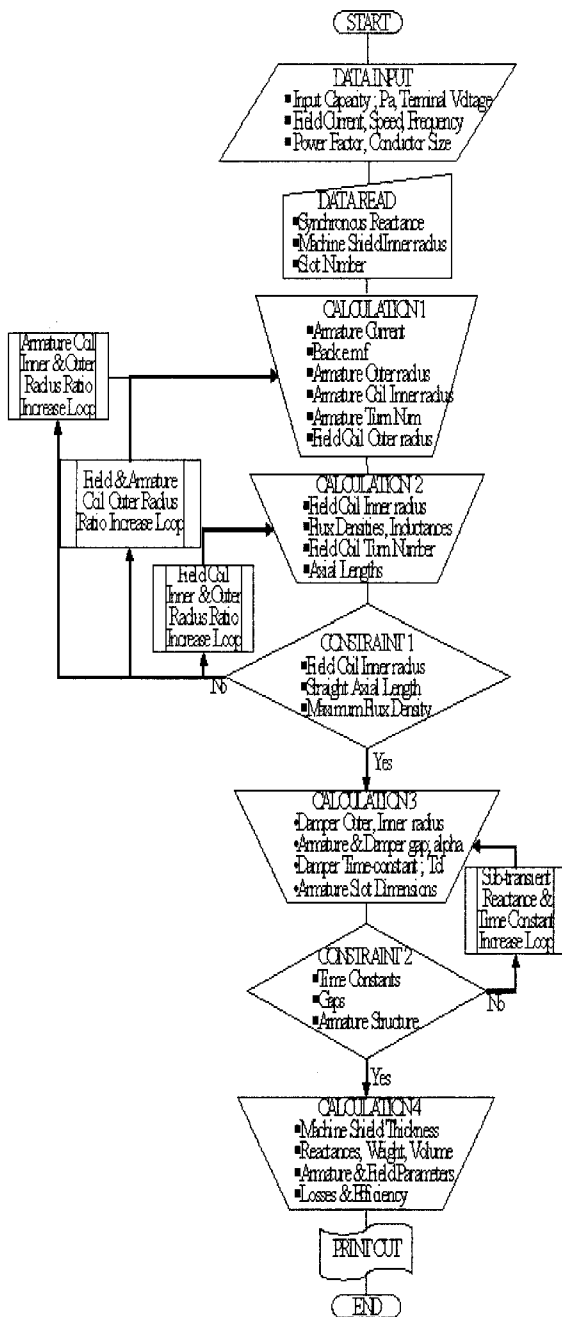


Fig. 2. Design program flow-chart of the air-cored type superconducting motor.

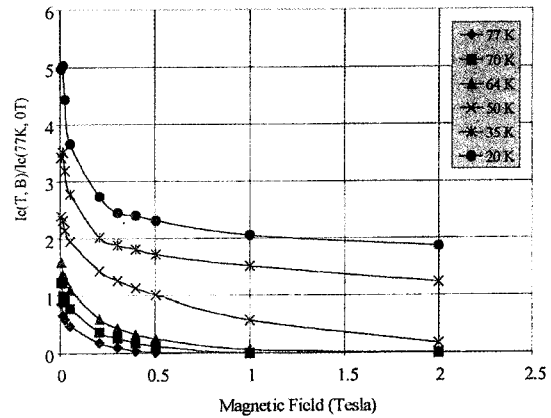


Fig. 3. Perpendicular magnetic field versus critical current curves of HTS wire for a 5 MW HTS motor design.

A 5 MW air-cored type HTS motor is designed with the design program described in Fig. 2. A design program result is focused on consuming expensive HTS wire as little as possible and getting high efficiency over 96 %. By running the design program several times, a proper program result was selected as shown in Fig. 4 where all the results are shown in case of 6 poles. More pole cases have shown results having larger HTS coil length and lower efficiency than 6 pole case. Table I shows the specification from the selected result and Fig. 5 shows the cross-section view. About 67 km HTS wire is needed in this air-cored type 5 MW class HTS motor, which increases production cost excessively and decreases cost competitiveness against conventional motor.

Table I. Design specification of Rotating field type 5 mw HTS Motor.

Rating Capacity	5 MW
Rating Speed	180 rpm
Pole Number	6
Armature Terminal Voltage	6600 V
Power Factor	1.0
Frequency	9 Hz
Synchronous Reactance	0.3 p.u.
Field Coil Rating Current	150 A
Field Coil Turn Number	3570 turns/pole
HTS wire Specification	Bi-2223 (4.2 x 0.31 mm) Ic = 125 A or 135 A @ 77 K, sf (AMSC Co.)
HTS wire Length	67 km
Armature Rating Current	464 A
Armature Turn Number	144 turns/phase
Armature Slot Number	72
Straight Axial Length	1110 mm
Machine Outer Diameter	1800 mm
Design Efficiency	96.22 %

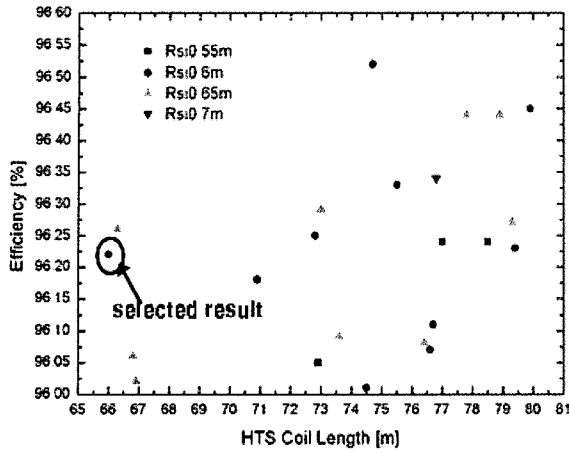


Fig. 4. A proper design program result selection among the results satisfying the design program of Fig. 2.

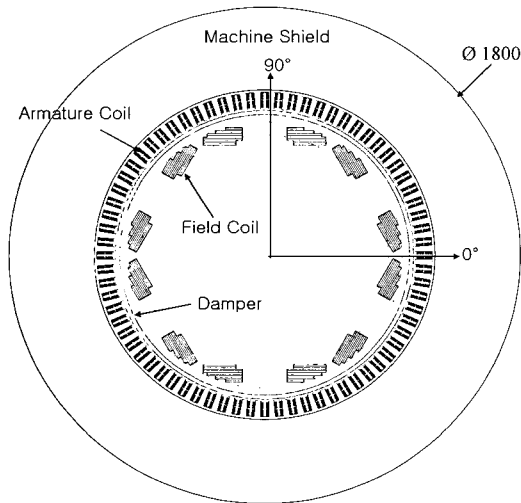


Fig. 5. Cross-sectional view of 5 MW air-cored type HTS motor, Case I (mm dimension).

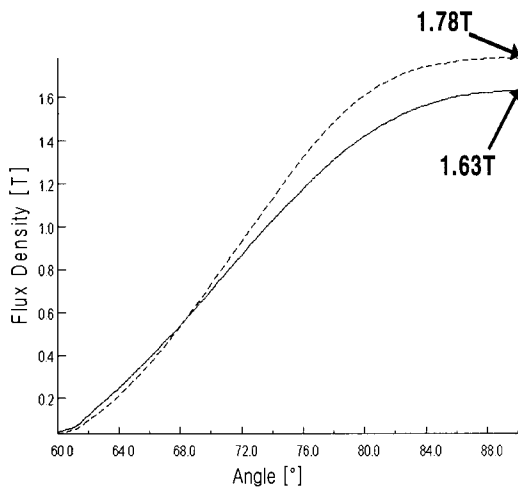


Fig. 6. Radial direction magnetic flux density distribution along the armature coil middle (continuous line) and inner radius (dashed line) in the air core type.

Fig. 6 shows radial direction magnetic field ( $B_r$ ) distribution along the inner and the middle radius of the armature coil of Fig. 5 via 2 dimensional Finite Element Method (FEM) analysis when the field coil is excited with rating current. This radial magnetic field distribution decides excitation voltage waveform that is expected to be so sinusoidal. The maximum flux density is 3.3 T and the maximum flux density crossing perpendicularly to HTS tape surface is 2.1 T at the field coil section.

## 2.2. Iron Core Inserted Type Design

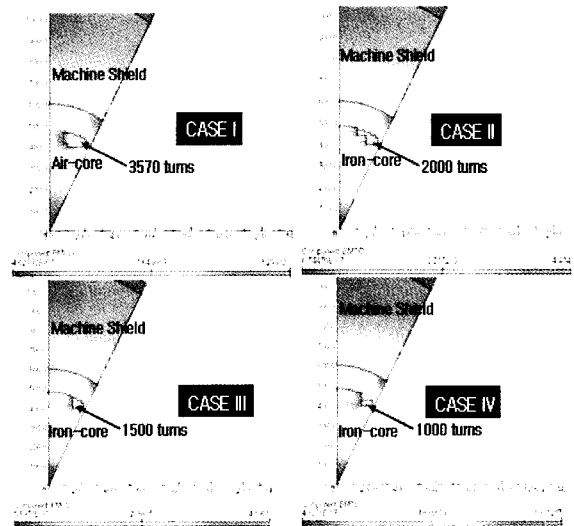


Fig. 7. FEM models to analyze iron core insertion effect.

Based on the air-core type design shown in Fig. 5, iron cores are inserted to reduce manufacturing cost by decreasing expensive HTS wire amount. As shown in the FEM models of Fig. 7, the HTS field coil section becomes smaller and smaller from the air-core type (Case I) to the iron-core type (Case IV). FEM analysis is done 2 dimensionally with the field excited with rating current, 150 A. The inserted iron core is given with the same B-H curve as the machine shield as shown in Fig. 8[4].

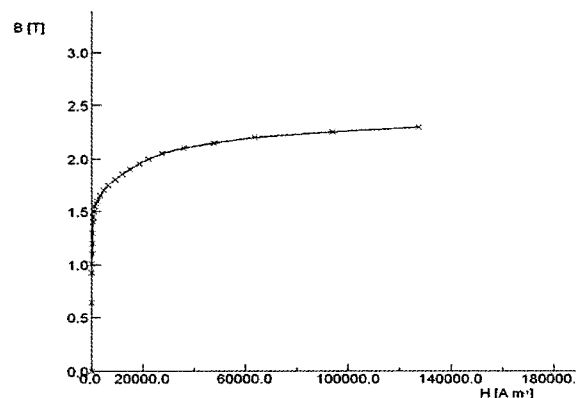


Fig. 8. B-H curve used for machine shield and inserted iron core.

The maximum flux ( $\Phi_{\max}$ ) linked with one phase armature coil can be calculated by integration of radial flux density ( $B_r$ ) along the armature coil middle radius. From this analysis  $\Phi_{\max}$  is calculated along the straight axial length ( $l$ ) of field coil. In case of air core type,  $B_r$  distribution along the armature coil is shown in Fig. 6 and  $\Phi_{\max}$  is calculated from the equation (1) as 0.6493 Wb along the armature coil middle radius,  $R_{\text{arm}}$ , and through the axial straight length,  $l$ , which is 1110 mm. Line to line excitation voltage (generated armature voltage by field coil rotation) can be calculated from equation (2), where  $\omega$  is angular frequency and  $N_{ph}$  is armature coil turn number per phase. This voltage is very much important because it decides amount of output power of a synchronous motor and torque waveform.

The air core type, Case I, generates 6476 V line to line excitation voltage and other cases are also calculated as listed in table II for the same straight axial length with Case I.

$$\Phi_{\max} = 2lR_{\text{arm}} \int_{60^\circ}^{90^\circ} B_r d\theta \quad (1)$$

$$V_{\text{exc}} = \frac{\sqrt{3}\omega\Phi_{\max}}{\sqrt{2}} N_{ph} \quad (2)$$

Fig. 9 shows radial magnetic field distributions along the armature in Case II. The flux density is larger than Case I so the straight axial length can be reduced from 1110 mm to 814 mm in order to get 100 % (6476 V) excitation voltage. Furthermore HTS conductor length can be reduced from 66.6 km to 31.9 km by iron core insertion.

Table II. Case by case Analysis Result.

	Case I	Case II	Case III	Case IV
Iron Core Insertion	X	O	O	O
Turns per Pole	3570	2000	1500	1000
Excitation Voltage (Line to Line)	6476 [V] (100 %)	8836 [V] (136.4 %)	7995 [V] (123.5 %)	6374 [V] (98.4 %)
Straight Axial Length for 100 % Excitation Voltage	1110 [mm]	814 [mm]	899 [mm]	1128 [mm]
HTS Conductor Length for 100 % Excitation Voltage	66.6 [km]	31.9 [km]	26.3 [km]	20.4 [km]
Maximum Flux Density perpendicular to HTS Tape surface	2.10 [T]	2.43 [T]	2.73 [T]	2.09 [T]

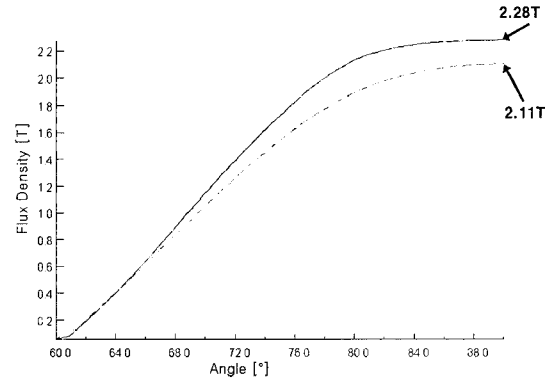


Fig. 9. Radial direction magnetic flux density distribution along the armature middle (continuous line) and inner radius (dashed line) in Case II.

Fig. 10 shows radial magnetic field distributions along the armature in Case III. The straight axial length can be reduced to 899 mm to get 100 % (6476 V) excitation voltage and HTS conductor length can be reduced more to 26.3 km than Case II by iron core insertion.

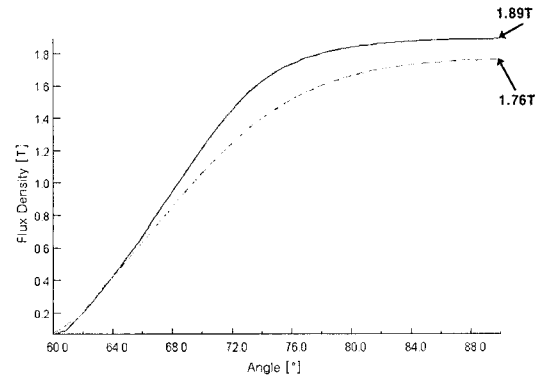


Fig. 10. Radial direction magnetic flux density distribution along the armature middle (continuous line) and inner radius (dashed line) in Case III.

Fig. 11 shows radial magnetic field distributions along the armature in Case IV. The straight axial length is extended a little from 1110 mm in Case I to 1128 mm to get 100 % (6476 V) excitation voltage but HTS conductor length is reduced more to 20.4 km by iron core insertion.

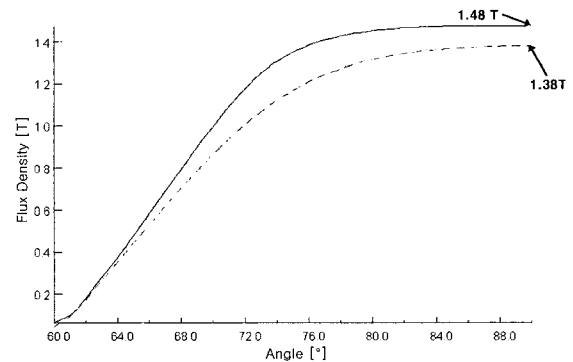


Fig. 11. Radial direction magnetic flux density distribution along the armature middle (continuous line) and inner radius (dashed line) in Case IV.

From the above results the HTS conductor length can be reduced via iron core while the axial length does not vary too much. So it is expected that machine efficiency does not vary too much either from the first design, Case I, by air-core type due to copper (joule) loss change at the armature coil by the axial length variation. The Case II and III are expected to get higher efficiency than Case I because of smaller axial length of armature coils and machine shield volume. Fig. 12 shows loss analysis result of the air-core type design, Case I, where the armature copper loss consists more than 2/3 of total loss.

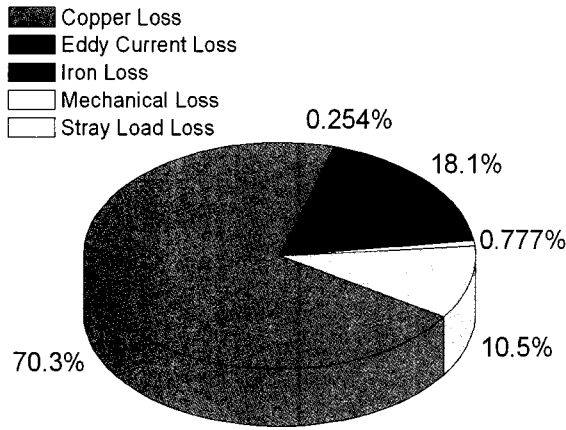


Fig. 12. Loss analysis result of the air-core type, Case I.

From the Case IV of iron-cored design, the final cross-section has been decided as shown in Fig. 13 where the machine shield outer diameter was modulated to get proper magnetic field in the machine shield and a 600 mm diameter bore was located in the center to reduce iron-core weight and arrange rotor shaft and cryogenic cooling means.

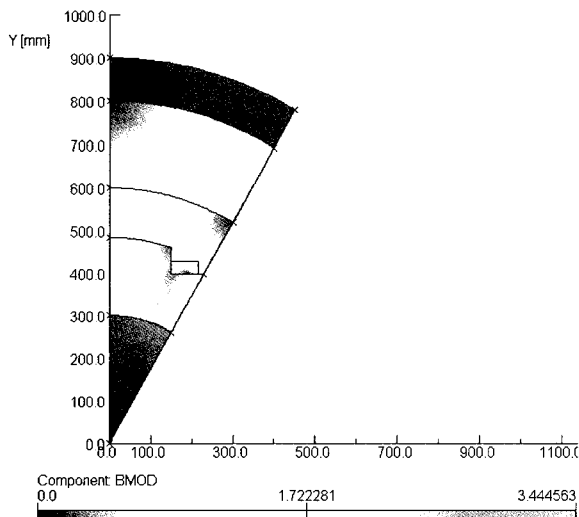


Fig. 13. Final design model of iron-cored type from Case IV.

Fig. 14 shows longitudinal cross-section view of the air-cored design, Case I. Fig. 15 shows longitudinal cross-section view of the final iron-cored design of Fig. 13. The final iron-cored design shows 200 mm smaller diameter but 117 mm larger axial length than the air-cored case. The iron-cored design shows better results such as smaller size, less weight and higher efficiency as shown in Table III. Even though the iron-cored design uses iron-core in the rotor, the total weight is lower than the air-cored design because the machine shield weight has been reduced more. As the same way the machine efficiency is higher due to the lower machine shield iron loss although the copper and stray losses get higher.

Table III. Comparison between Air-cored and Iron-cored Design.

Design Parameters		Air-cored Design	Iron-cored Design
Volume [m <sup>3</sup> ]		4.58	3.82
Weight [kg]	Machine Shield	16350	9896
	Iron Core	0	5608
	Damper	662	709
	Field Coil	648	198
	Armature Coil	320	337
	Etc (Cooling System & Support Structure)	10000 (Approx.)	9000 (Approx.)
	<b>Total Weight</b>	<b>27980</b>	<b>25748</b>
Losses [kW]	Armature Copper (Joule) Loss	140.96	148.38
	Machine Shield Iron Loss	36.28	24.29
	Stray Load Loss	21.14	22.26
	Mechanical Loss	1.56	1.56
	Eddy Current Loss	0.51	0.51
	<b>Total Loss</b>	<b>200.45</b>	<b>197</b>
Efficiency [%]		96.22	96.27
HTS Conductor Length [km]		66.6	20.4

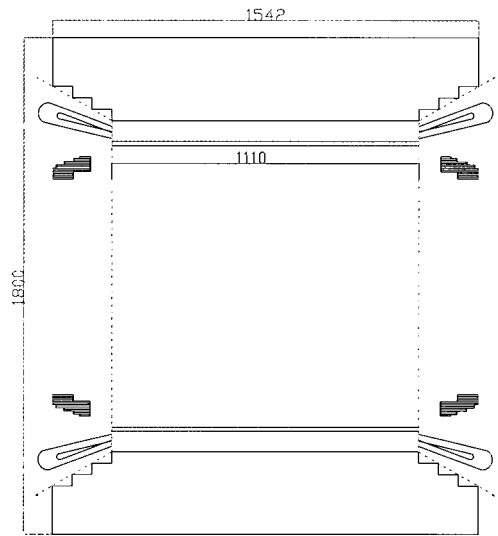


Fig. 14. Longitudinal cross-section view of a 5 MW air-cored type design HTS motor, Case I (mm dimension).

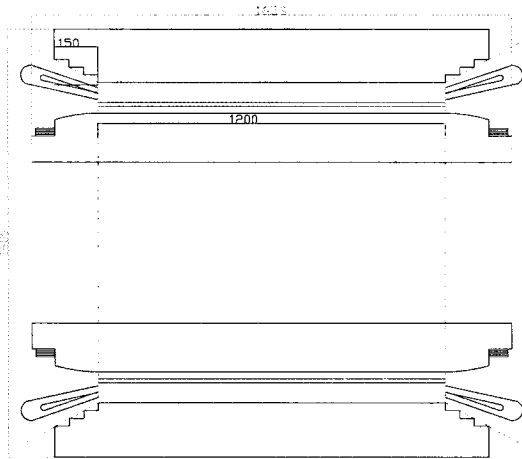


Fig. 15. Longitudinal cross-sectional view of a 5 MW iron-cored type design HTS motor from Fig. 13 (mm dimension).

### 3. CONCLUSION

In this paper a 5 MW rotating field type HTS synchronous motor had been designed firstly based on air core type using a design program coded with equations obtained from mathematical 2 dimensional magnetic field analysis. In order to reduce expensive HTS wire consumption, it has been designed by inserting iron core within the field coil section. It is figured out that the iron-core inserting design can reduce required HTS wire length to about 1/3 of the original air-core type design. By using 2 dimensional FEM analysis, excitation voltages could be calculated in several cases of iron-core insertion and compared with the original air-cored case. Through the analysis the iron-core cases have the same excitation voltage with the air-core type even with smaller axial length and show better results smaller size, less weight and higher efficiency. Although the design approach in this paper is based on 2 dimensional analysis, the design parameters such as excitation voltage and coil inductances can be calculated more precisely through 3 dimensional analysis.

### ACKNOWLEDGMENT

This research was supported by a grant from Center for Applied Superconductivity Technology of the 21st Century Frontier R&D Program funded by the Ministry of Education, Science and Technology, Republic of Korea.

### REFERENCES

[1] Greg Snitchler, et al, "The Performance of a 5 MW High Temperature Superconductor Ship

Propulsion Motor," IEEE TRANSACTIONS ON APPLIED SUPERCONDUCTIVITY, Vol.15, No. 2, JUNE 2005.

[2] S.K. Baik, et al, "Effect of Synchronous Reactance and Power Factor on HTS Synchronous Machine Design and Performance," IEEE TRANSACTIONS ON APPLIED SUPERCONDUCTIVITY, Vol.16, No.2, JUNE 2006.  
 [3] S.K. Baik, et al, "Design of Water-cooled 1MW HTS Synchronous Motor," Journal of The Korea Institute of Applied Super conductivity and Cryogenics, Vol. 7, No.3, Sep. 2005.  
 [4] "OPERA-2D REFERENCE MANUAL," Vector Fields Limited, Version 8.0, March, 2001.

### 저 자 소 개



**백승규(白承珪)**

1972년 11월 19일생, 1995년 부산대학교 전기공학과 졸업, 1997년 동대학원 전기공학과 졸업(공학석사), 현재 동대학원 전기공학과 박사과정, 한국전기연구원 초전도기기 연구그룹 선임연구원.



**권영길(權永吉)**

1959년 7월 28일생, 1982년 부산대학교 기계공학과 졸업, 1984년 동대학원 기계공학과 졸업(공학석사), 1990년 동대학원 기계공학과 졸업(공학박사), 1990~1991년 한국기계연구원 선임연구원, 현재 한국전기연구원 초전도기기 연구그룹 그룹장.



**김호민(金鎬民)**

1970년 8월 23일생, 1995년 제주대학교 전기공학과 졸업, 1998년 연세대학교 대학원 전기공학과 졸업(공학석사), 2002년 동대학원 전기전자공학과 졸업(공학박사), 2002년~2004년 M.I.T. Francis Bitter Magnet Lab. Post-Doctoral Research Associate, 2004년~2007년 LG 산전(주) 전력연구원 선임연구원, 현재 한국전기연구원 초전도기기 연구그룹 선임연구원.



**이재득(李在得)**

1975년 9월 7일생, 2001년 창원대학교 공과대학 전기공학과 졸업, 2003년 동대학원 전기공학과 졸업(공학석사), 현재 동대학원 전기공학과 박사과정, 한국전기연구원 초전도기기 연구그룹 위촉연구원.



**김영춘(金永春)**

1964년 12월 26일생, 1986년 금오공과대학교 기계공학과 졸업, 1991년 동대학원 기계공학과 졸업(공학석사), 2004년 한국과학기술원 기계공학과 졸업(공학박사), 현재두산중공업(주) 기술연구원 책임연구원.



박희주(朴希柱)

1970년 9월 25일생, 1995년 한국해양대학교 기계공학과 졸업, 1997년 동대학원 기계공학과 졸업(공학석사), 현재 두산중공업(주) 기술연구원 주임연구원.



권운식(權叢植)

1976년 2월 2일생, 1998년 경상대 공과대학 기계공학과 졸업, 2004년 동 대학원 기계공학과 졸업(공학석사), 2002년~2004년 한국전기연구원 초전도응용연구그룹 위촉연구원, 현재 두산중공업(주) 기술연구원 주임연구원.



박관수(朴寬秀)

1963년 3월 25일생, 1985년 서울대 공과대학 전기공학과 졸업, 1987년 동 대학원 전기공학과 졸업(공학석사), 1992년 동대학원 전기공학과 졸업(공학박사), 1992~1993년 서울대학교 공학 연구소 특별 연구원, 1994~2003년 한국해양대학교 부교수, 2003~2005년 부산대학교 조교수, 현재 부산대학교 전자 전기 정보 컴퓨터 공학부 부교수.